Supporting Information

Dumbbells of five-connected silicon atoms and superconductivity in the binary silicides MSi_3 (M = Ca, Y, Lu)

Ulrich Schwarz, Aron Wosylus, Helge Rosner, Walter Schnelle, Alim Ormeci, Katrin Meier, Alexey Baranov, Michael Nicklas, Susann Leipe, Carola J. Müller, and Yuri Grin*

Max-Planck-Institut für Chemische Physik fester Stoffe, Nöthnitzer Str. 40, 01187 Dresden,

Germany

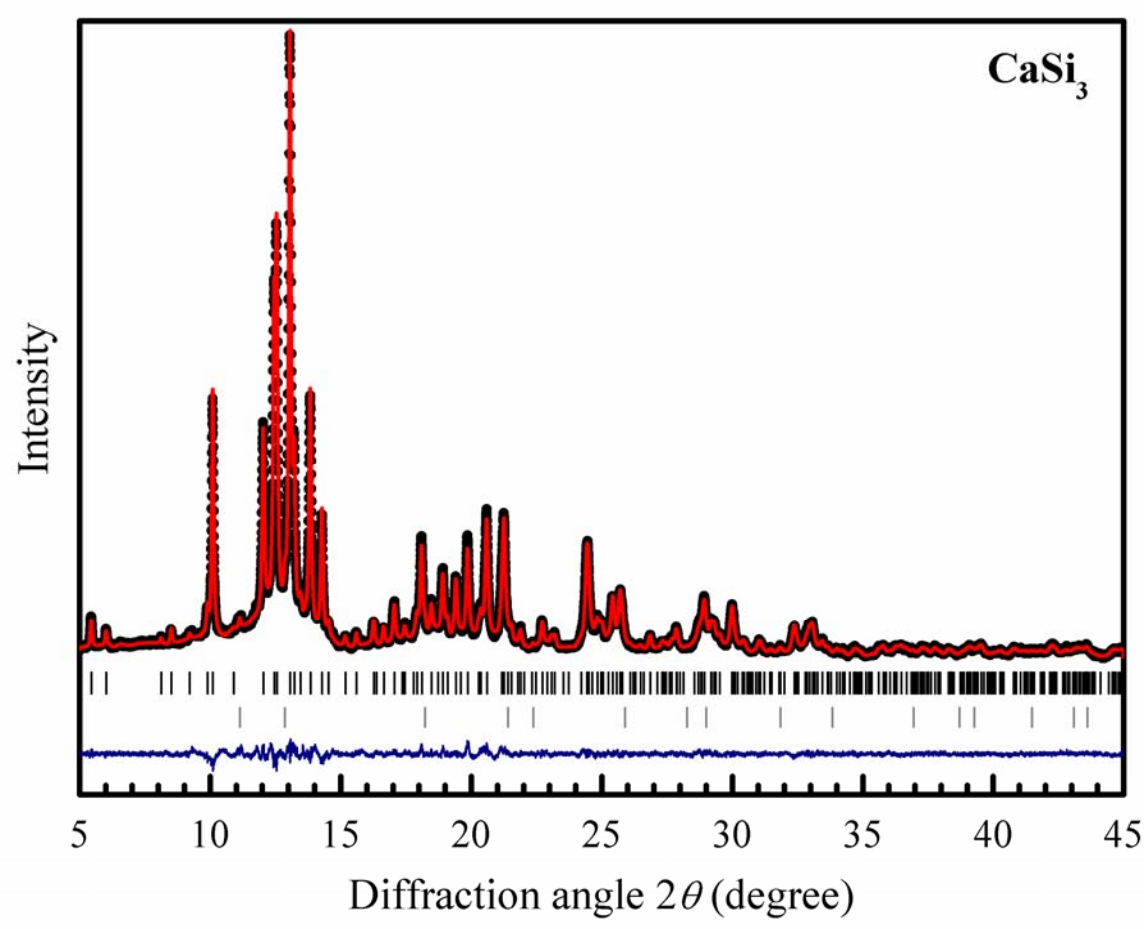

Figure S1. Top: Diffraction pattern of $CaSi_3$ collected at room temperature with synchrotron radiation (λ = 53.837 pm) at beamline B2 of the DESY/Hasylab. Reflection positions are marked by vertical ticks (top: black: $CaSi_3$, grey: CaO), the observed pattern is displayed as black points, the calculated patterns as a red curve. The differences between observed and calculated intensities are shown in blue.

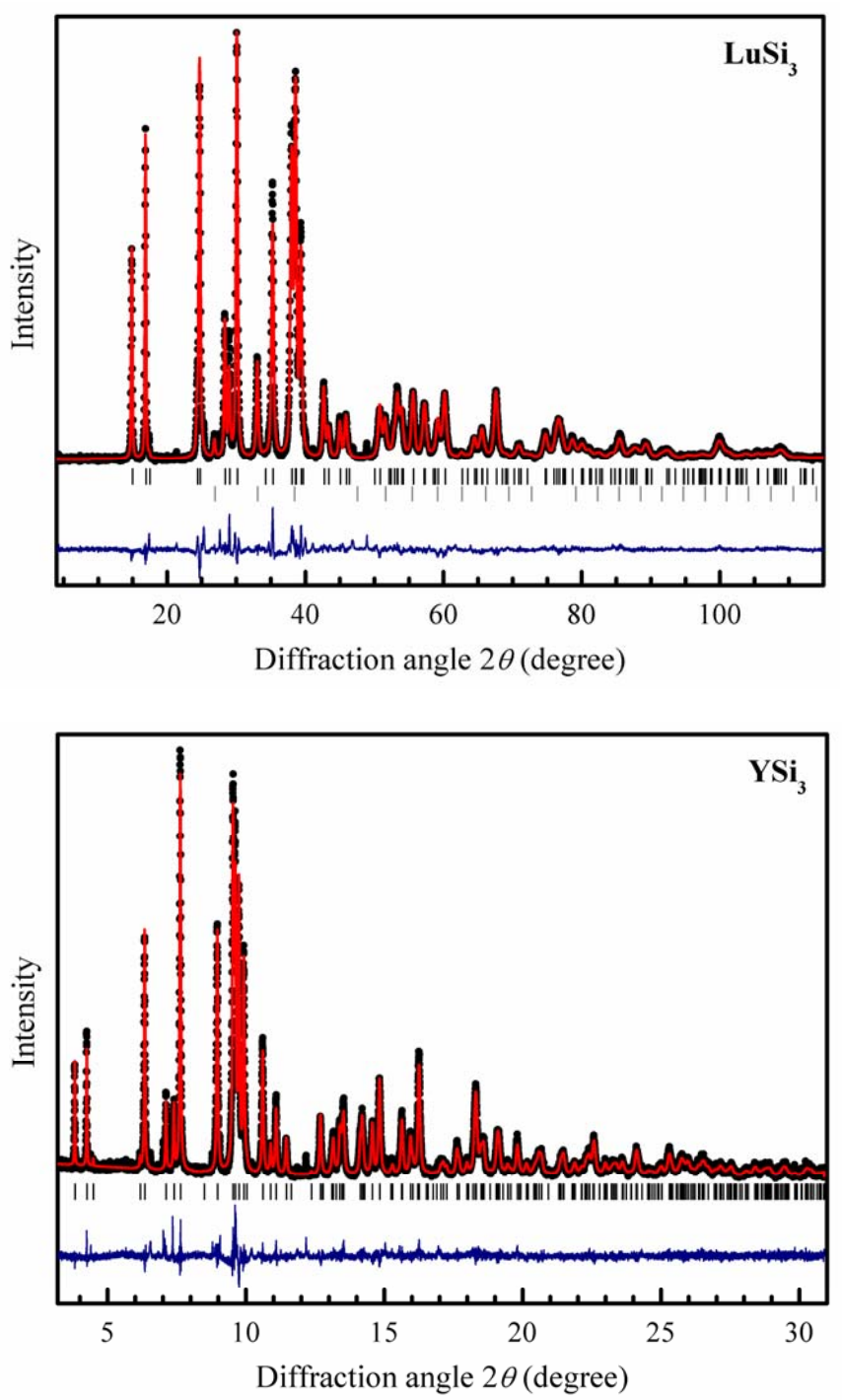

Figure S2. Diffraction patterns of $LuSi_3$ (top) and YSi_3 (bottom) at ambient conditions. Data of $LuSi_3$ were collected with a sealed laboratory source (STOE-STADIP-MP) in reflection alignment (λ = 154.060 pm) and those of YSi_3 with synchrotron radiation (λ = 39.987 pm) at beamline ID31 of the ESRF. Peak positions are marked by vertical ticks (top: black: $LuSi_3$, grey: Si(*cI*16); bottom: black: YSi_3), the background-corrected patterns are displayed as black points, the calculated patterns as red curves. The differences between observed and calculated intensities are shown in blue.

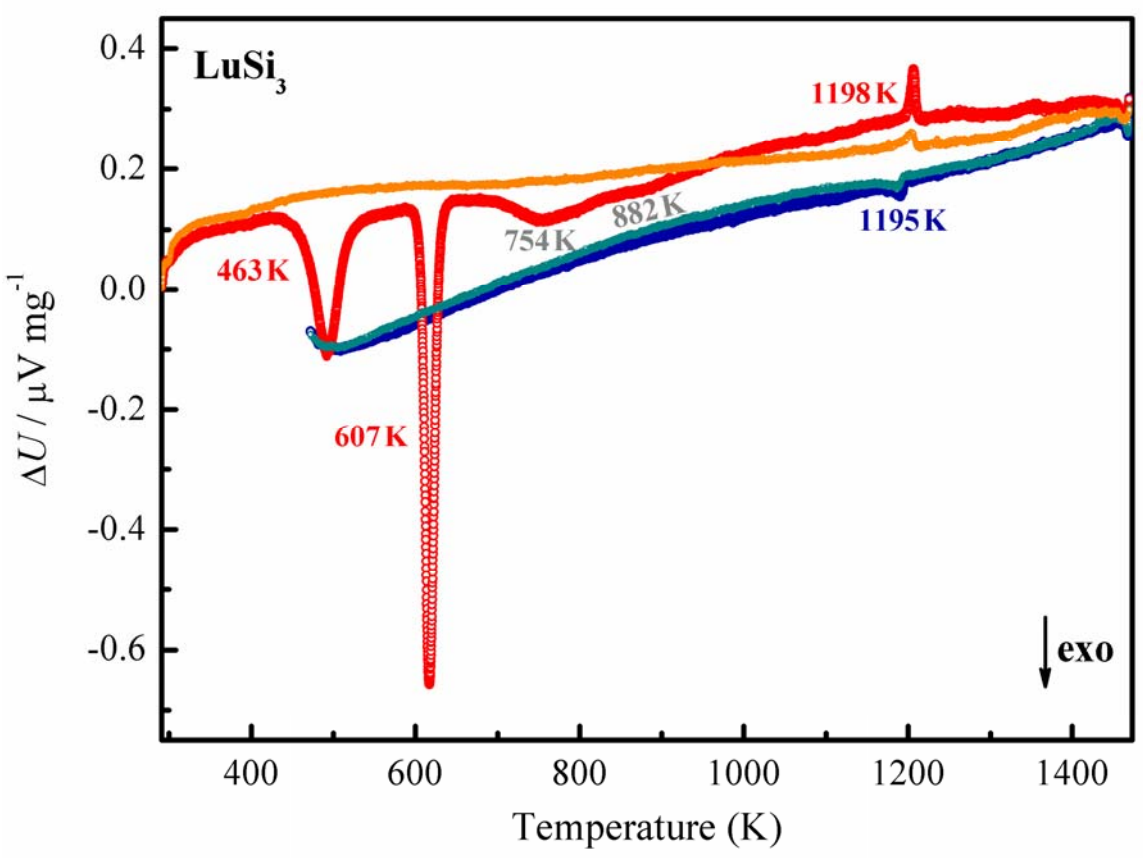

Figure S3. Differential scanning calorimeter measurements of a sample with nominal composition $Lu_{16}Si_{87}$, i.e., a mixture of $LuSi_3$ and Si(*cI*16) in the mass ratio 80:20, versus temperature. The first heating is indicated red, the second one orange. Blue and dark cyan indicate the first and second cooling process, respectively. The first exothermic signal at 463 K is attributed to the irreversible transformation Si(*cI*16) to diamond-type Si(*cF*8), the second exothermic effect at 607 K to the monotropic decomposition of $LuSi_3$. This evidence suggests that $LuSi_3$ is metastable at ambient pressure.

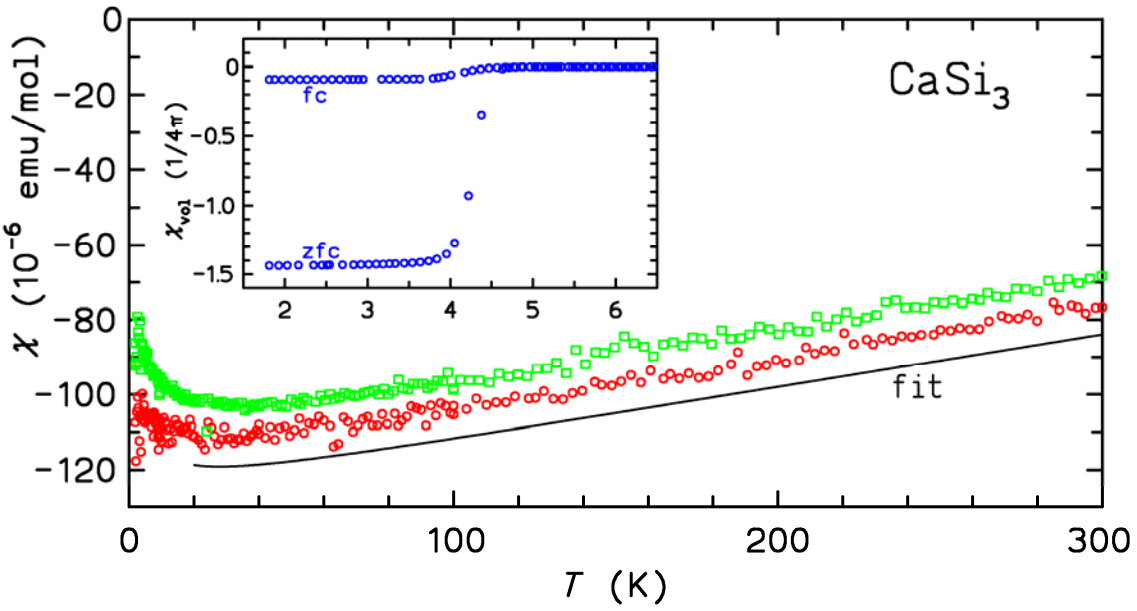

Figure S4. Magnetic susceptibility $\chi(T)$ of the $CaSi_3$ sample in $\mu_0 H = 3.5$ T (green squares), 7.0 (red circles) and fit to the extrapolated data (black line). The inset shows the superconducting transition in the zero field cooled (zfc) and field cooled (fc) susceptibility for the nominal field $\mu_0 H = 2$ mT.

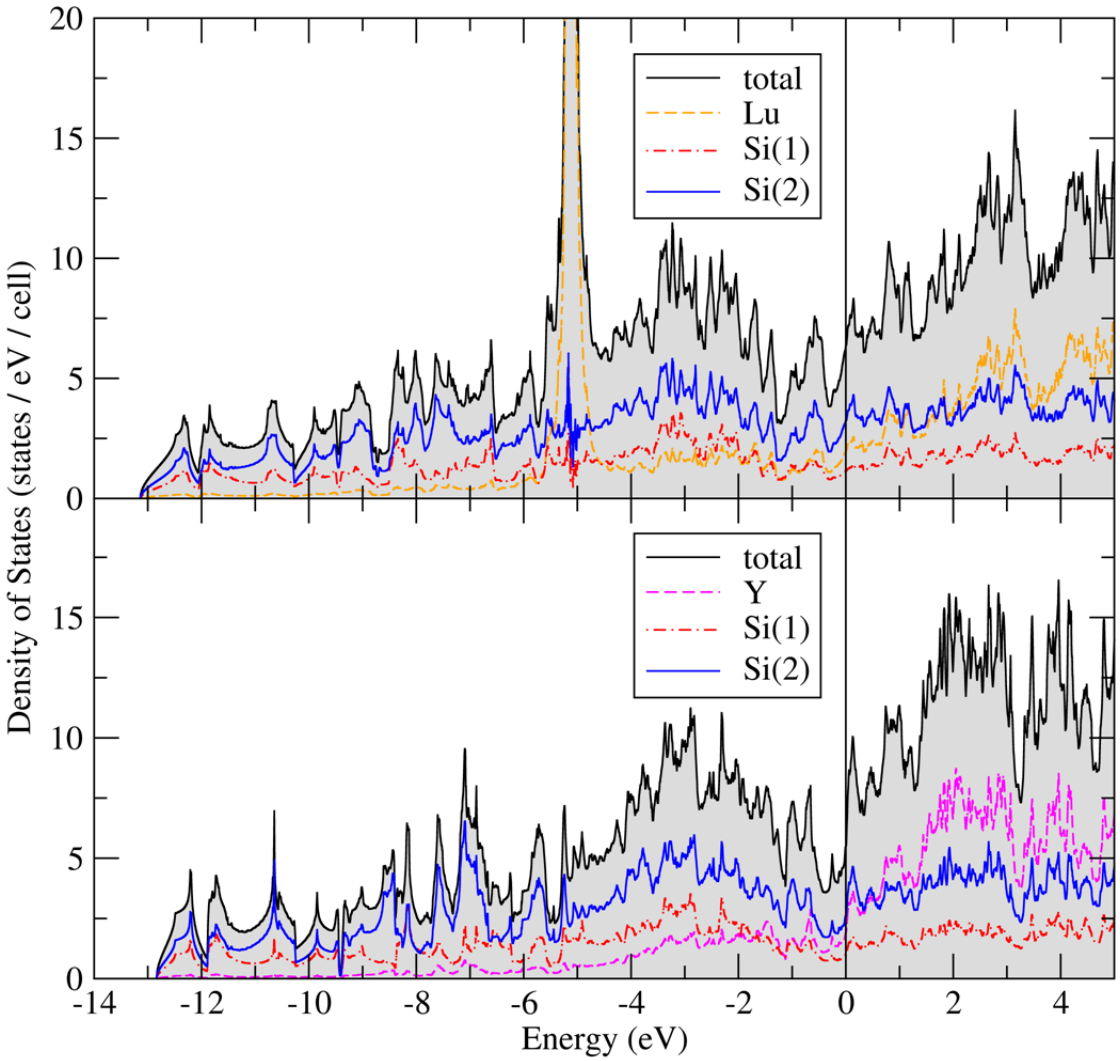

Fig. S5. Electronic density of states with partial contributions of the metal and the silicon atoms of $LuSi_3$ (top) and YSi_3 (bottom). The Fermi level is located at zero energy. Disregarding the localized Lu 4f states at approximately -5 eV, both the total and the partial DOS evidence the pronounced similarity of especially the metal contributions.

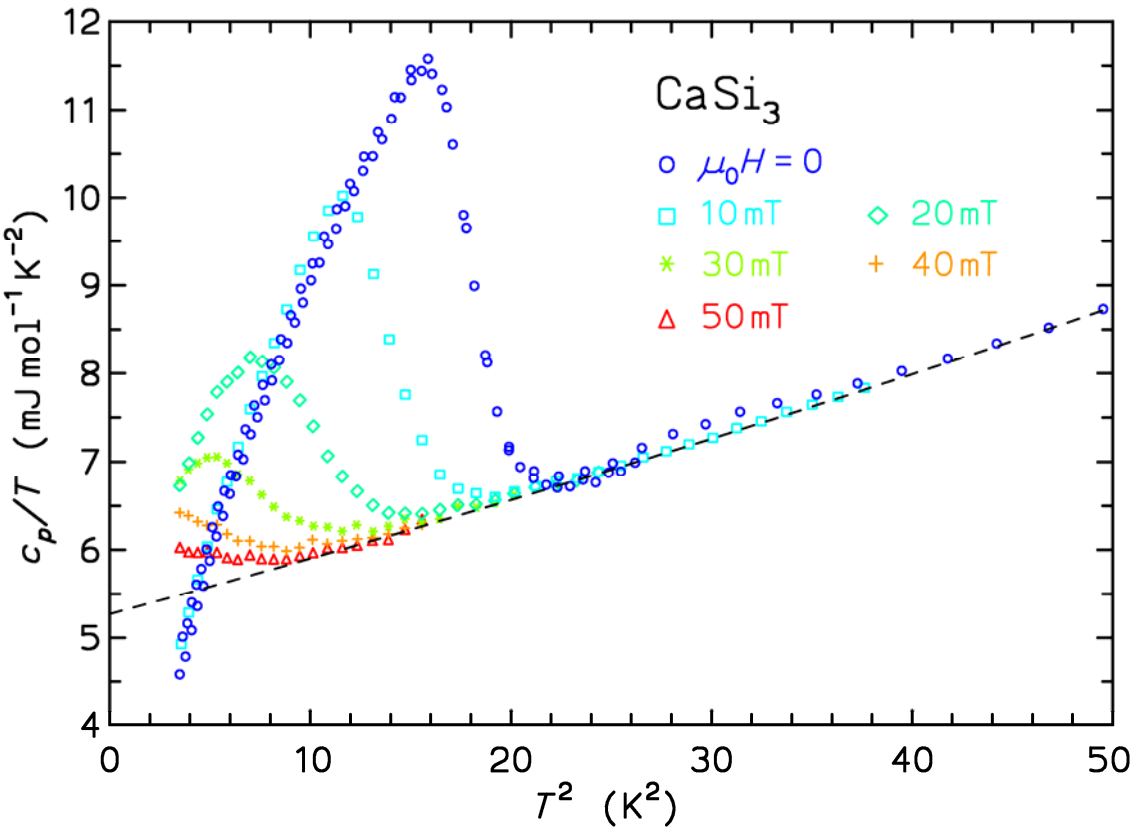

Figure S6. Molar heat capacity $c_p(T,H)/T$ of $CaSi_3$ versus T^2 for magnetic fields between zero and 50 mT. The dashed black line displays the fit to the normal-state specific heat.

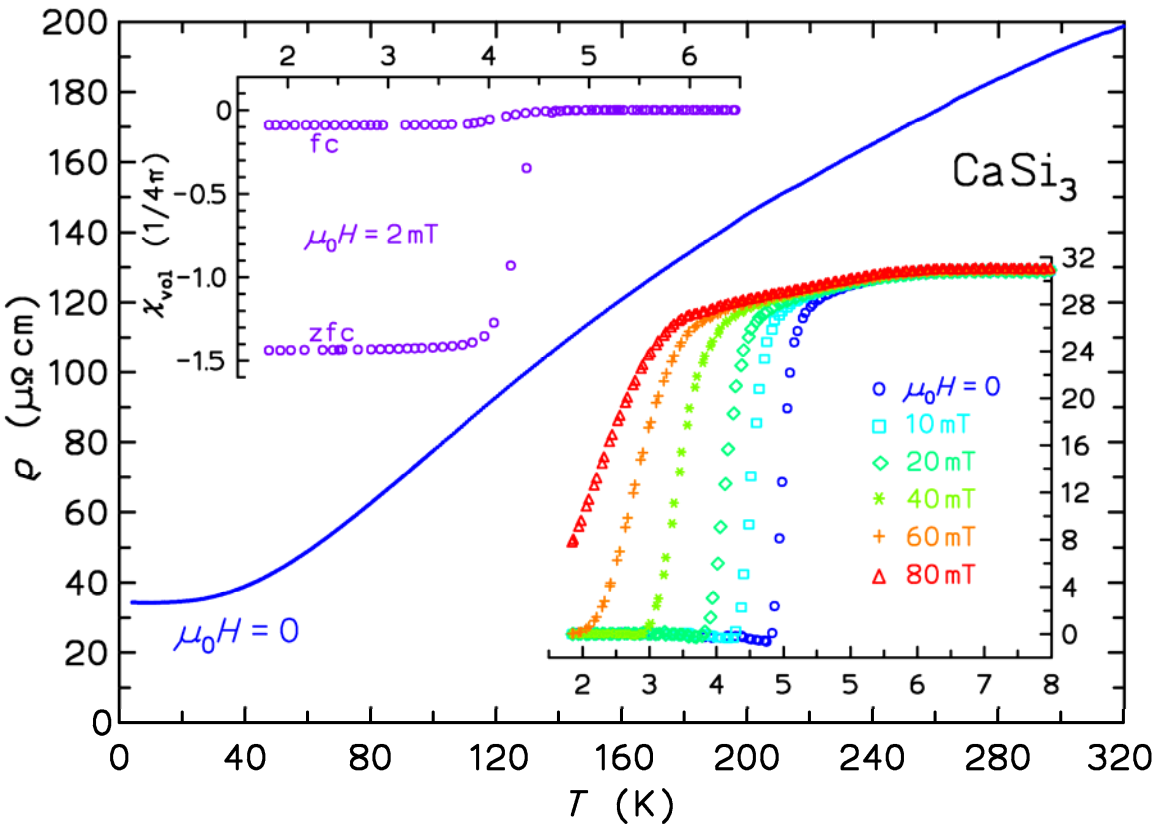

Figure S7. Electrical resistance ρ of $CaSi_3$ versus temperature T. The lower right inset shows the region of the superconducting transition for magnetic fields between zero and 80 mT. The upper left inset shows measurements of the magnetic susceptibility in field cooling (fc) and after zero-field cooling (zfc) evidencing the Meißner effect and the shielding.

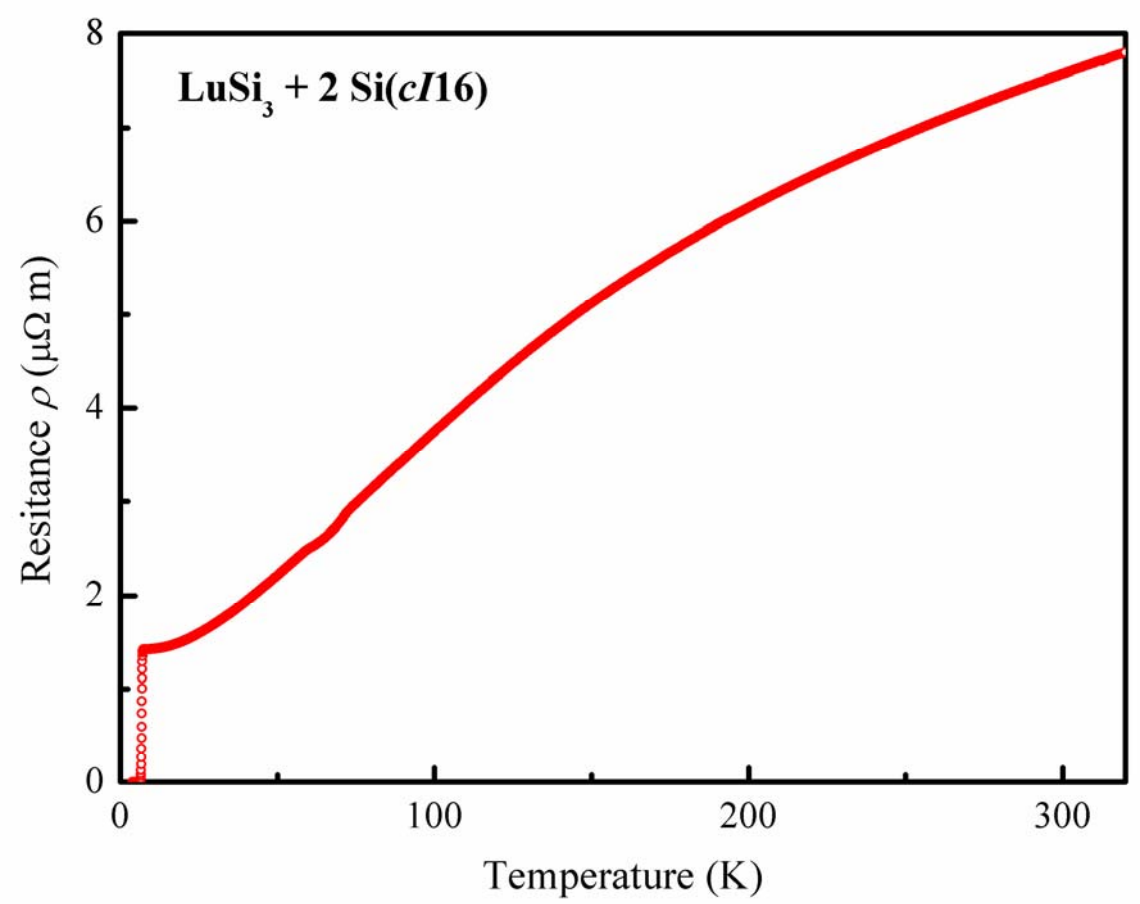

Figure S8. Electrical resistance ρ of a sample with nominal composition $Lu_{16}Si_{87}$, i.e., a mixture of $LuSi_3$ and Si(*cI*16) in the mass ratio 80:20, versus temperature *T*. The high absolute values in the metal-like regime are attributed to grain boundary effects. The steep decrease at low temperatures originates from the superconducting transition in $LuSi_3$.

Table S1a. Details of the powder X-ray diffraction measurement and Rietveld refinement of the crystal structure of $CaSi_3$.

Formula	$CaSi_3$
Crystal system, space group	tetragonal, *I*4/*mmm* (no. 139)
Cell parameters	Refinement with LaB_6, CuKα1-radiation (λ = 154.0562 pm) from $3° \le 2\theta \le 100°$ using 26 reflections of the sample a = 726.76(4) pm c = 1135.01(7) pm $V = 599.49(6) \times 10^6$ pm^3
Formula units per cell	$Z = 8$
Calculated density	$\rho_{calc} = 2.76$ g cm^{-3}
Crystal dimensions	powder
Temperature / K	293(2)
Measurement device	Beamline B2 of HASYLAB at DESY glass capillary with a diameter of 0.5 mm on-site readable image plate detector OBI[1] step width: 0.004°
Radiation	Synchrotron, λ = 53.837 pm
Function for profile fitting	Thompson-Cox-Hastings pseudo-Voigt with axial divergence asymmetry[2]
Measurement limits	$2.0° \le 2\theta \le 67.5°$ refinement limits: $5.0° \le 2\theta \le 45°$ $0 \le h \le 10$, $0 \le k \le 7$, $0 \le l \le 16$
Number of points/ reflections	10000 / 300
Number of parameters crystal structure/ background and profile	10 / 79
Structure refinement	Rietveld method implemented in the program package FullProf-Suite[3]
Figures of merit	$R_p = 0.029$, $R_{wp} = 0.036$, , $R_{exp} = 0.009$

[1] M. Knapp, V. Joco, C. Baehtz, H. H. Brecht, A. Ehrenberg, H. Seggern, H. Fuess, *Nucl. Instrum. Methods A* **2004**, *521*, 565

[2] P. Thompson, D. E. Cox, J. B. Hastings, *J. Appl. Cryst.* **1987**, *20*, 79
L. W. Finger, *J. Appl. Cryst.* **1998**, *31*, 111

[3] J. Rodriguez-Carvajal, *Physica B* **1993**, *192*, 55
J. Rodriguez-Carvajal, *Commission on Powder Diffraction (IUCr) Newsletter* **2001**, *26*, 12
J. Rodriguez-Carvajal, T. Roisnel, *International Union for Crystallography Newsletter* **1998**, *20*
T. Roisnel, J. Rodriguez-Carvajal, *Proceedings of the Seventh European Powder Diffraction Conference (EPDIC 7)* **2000**, 118

Table S1b. Positional and thermal displacement parameters of $CaSi_3$ as refined from powder X-ray diffraction data.

Atom	Wyckoff position	*x*	*y*	*z*	U_{iso} / 10^4 pm^2
Ca1	4*e*	0	0	0.17384(7)	0.0099(2)
Ca2	4*d*	½	0	¼	0.0113(2)
Si1	8*i*	0.3356(1)	0	0	0.0066(2)
Si2	16*m*	0.31399(6)	*x*	0.10589(5)	0.0121(2)

Table S1c: Selected interatomic distances of $CaSi_3$

Ca1 –	4 × Si1	313.72(8)
	4 × Si2	314.73(8)
	4 × Si2	331.80(5)
Ca2 –	4 × Si1	307.88(3)
	8 × Si2	311.61(5)
Si1 –	1 × Si1	239.0(1)
	4 × Si2	258.39(5)
	2 × Ca2	307.88(3)
	2 × Ca1	313.72 (8)
Si2 –	1 × Si2	240.37(8)
	2 × Si1	258.39(5)
	2 × Si2	270.37(6)
	2 × Ca2	311.61(5)
	1 × Ca1	314.73(8)
	1 × Ca1	331.80(5)

Table S2a. Details of the powder X-ray diffraction measurement and Rietveld refinement of the crystal structure of YSi_3.

Formula	YSi_3
Crystal system, space group	tetragonal, *I*4/*mmm* (no. 139)
Cell parameters	Refinement with LaB_6, CuKα1-radiation (λ = 154.0562 pm) from $3° \le 2\theta \le 100°$ using 29 reflections of the sample a = 723.10(3) pm c = 1079.2(1) pm $V = 564.29(6) \times 10^6$ pm^3
Formula units per cell	Z = 8
Calculated density	ρ_{calc} = 4.07 g cm^{-3}
Crystal dimensions	powder
Temperature / K	293(2)
Measurement device	ESRF ID31, glass capillary with a diameter of 0.3 mm Detector: counting tube, step width: 0.002°
Radiation	Synchrotron, λ = 39.987 pm
Function for profile fitting	Pseudo-Voigt
Measurement limits	$0.5° \le 2\theta \le 33°$ refinement limits: $3.2° \le 2\theta \le 30.9°$ $0 \le h \le 9$, $0 \le k \le 6$, $0 \le l \le 14$
Number of points/ reflections	13850 / 236
Number of parameters crystal structure/background and profile	10 / 16
Structure refinement	Rietveld method implemented in the program package FullProf-Suite[1]
Figures of merit	R_p = 0.083, R_{wp} = 0.115, , R_{exp} = 0.101

[1] J. Rodriguez-Carvajal, *Physica B* **1993**, *192*, 55
J. Rodriguez-Carvajal, *Commission on Powder Diffraction (IUCr) Newsletter* **2001**, *26*, 12
J. Rodriguez-Carvajal, T. Roisnel, *International Union for Crystallography Newsletter* **1998**, *20*
T. Roisnel, J. Rodriguez-Carvajal, *Proceedings of the Seventh European Powder Diffraction Conference (EPDIC 7)* **2000**, 118

Table S2b. Positional and thermal displacement parameters of YSi_3 as refined from powder X-ray diffraction data.

Atom	Wyckoff position	*x*	*y*	*z*	U_{iso} / 10^4 pm^2
Y1	4*e*	0	0	0.17050(9)	0.0066(3)
Y2	4*d*	½	0	¼	0.0063(3)
Si1	8*i*	0.3295(3)	0	0	0.0102(5)
Si2	16*m*	0.3141(1)	*x*	0.1117(1)	0.0110(4)

Table S2c. Selected interatomic distances of YSi_3

Y1 –	4 × Si1	301.04(6)
	4 × Si2	302.3(1)
	4 × Si2	327.41(8)
Y2 –	4 × Si1	296.63(9)
	8 × Si2	303.20(8)
Si1 –	1 × Si1	246.6(3)
	4 × Si2	257.37(8)
	2 × Y2	296.63(9)
	2 × Y1	301.0(2)
Si2 –	1 × Si2	241.1(2)
	2 × Si1	257.37(8)
	2 × Si2	268.9(1)
	1 × Y1	302.3(1)
	2 × Y2	303.20(8)
	1 × Y1	327.41(8)

Table S3a. Details of the powder X-ray diffraction measurement and Rietveld refinement of the crystal structure of $LuSi_3$.

Formula	$LuSi_3$
Crystal system, space group	tetragonal, *I*4/*mmm* (no. 139)
Cell parameters	Refinement with LaB_6, CuKα1-radiation (λ = 154.0562 pm) from 3° ≤ 2θ ≤ 100° using 26 reflections of the sample a = 718.35(8) pm c = 1047.1(1) pm V = 540.3(1) × 10^6 pm^3
Formula units per cell	Z = 8
Calculated density	ρ_{calc} = 6.37 g cm^{-3}
Crystal dimensions	powder
Temperature / K	293(2)
Measurement device	STOE-STADIP-MP Ge-Monochromator, Debye-Scherrer geometry, reflexion alignment, step width: 0.02°
Radiation	CuKα1, λ = 154.060 pm
Function for profile fitting	Pseudo-Voigt[1]
Measurement limits	4.0° ≤ 2θ ≤ 120° refinement limits: 4.0° ≤ 2θ ≤ 115° 0 ≤ h ≤ 7, 0 ≤ k ≤ 5, 0 ≤ l ≤ 11
Number of points/ reflections	5550 / 129
Number of parameters crystal structure/background and profile	10 / 23
Structure refinement	Rietveld method implemented in the program package GSAS[2]
Figures of merit	R_p = 0.054, R_{wp} = 0.076, , R_{exp} = 0.037, R_F = 0.033

[1] Pseudo-Voigt profile coefficients in TCH parameterization:
P. Thompson, D. E. Cox, J. B. Hastings, *J. Appl. Cryst.* **1987**, *20*, 79
Asymmetry correction:
L. W. Finger, D. E. Cox, A. P. Jephcoat, *J. Appl. Cryst.* **1994**, *27*, 892

[2] A. C. Larson, R. B. von Dreele, *General Structure Analysis System (GSAS)*, Los Alamos National Laboratory Report LAUR 86, **2004**
B. H. Toby, *J. Appl. Cryst.* **2001**, *34*, 210

Table S3b. Positional and thermal displacement parameters of $LuSi_3$ as refined from powder X-ray diffraction data.

Atom	Wyckoff position	*x*	*y*	*z*	U_{iso}[1] / 10^4 pm^2
Lu1	4*e*	0	0	0.1683(1)	0.0253(2)
Lu2	4*d*	½	0	¼	0.0254(2)
Si1	8*i*	0.3309(6)	0	0	0.027(1)
Si2	16*m*	0.3126(2)	*x*	0.1167(2)	0.0259(9)

Table S3c: Selected interatomic distances of $LuSi_3$

Lu1 –	4 × Si2	294.8(2)
	4 × Si1	295.90(7)
	4 × Si2	322.1(2)
Lu2 –	4 × Si1	288.6(2)
	8 × Si2	296.7(2)
Si1 –	1 × Si1	243.0(6)
	4 × Si2	256.0(2)
	2 × Lu2	288.6(2)
	2 × Lu1	295.9(4)
Si2 –	1 × Si2	244.4(3)
	2 × Si1	256.0(2)
	2 × Si2	269.2(2)
	1 × Lu1	294.8(2)
	2 × Lu2	296.7(2)
	1 × Lu1	322.1(2)

Table S4. Important physical parameters of the MSi$_3$ compounds in the normal and superconducting state: critical temperature of the superconducting state (T_c) from the midpoint of the specific heat anomaly, Debye temperature Θ_D and normal-state Sommerfeld coefficient of the electronic specific heat (γ_{exp}), computed (unrenormalized) electronic specific heat γ_{comp}, electron-phonon coupling parameter λ, ratios of the specific heat anomaly $\Delta c_p/T_c$ and $\Delta c_p/\gamma_N T_c$, estimated upper critical magnetic field ($\mu_0 H_{c2}$), onset critical temperature of the superconducting state ($T_{c,on}$) from the fc magnetic susceptibility in an external field $\mu_0 H$ = 2 mT, volume fraction V of Meissner flux expulsion (fc) and shielding (zfc) in the same field.

	CaSi$_3$	**YSi$_3$**	**LuSi$_3$** [1]
T_c/K	4.25	4.63	6.78
Θ_D/K	514	451	365
γ_{exp} /mJ mol^{-1} K^{-2} [2]	4.81 - 5.27	5.16	6.26
γ_{comp} /mJ mol^{-1} K^{-2}	3.0	3.3	3.8
λ [3]	0.6 - 0.8	0.6	0.65
$(\Delta c/T_c)$ / mJ mol^{-1} K^{-2}		7.6	9.4
$\Delta c_p/\gamma_N T_c$ [4]	1.05 – 1.17	1.42	1.50
$\mu_0 H_{c2}$/mT [4]	48(3)	80(3)	234(5)
$T_{c,on}$/K	4.50(5)	5.0(1)	7.1(1)
V_{zfc} [6]	1.4	1.4	2.1
V_{fc} [6] [7]	0.04 – 0.09	0.42	0.11

1) Corrected for the contributions of a Si(cI16) impurity (resistivity values as measured).
2) Calculated form the normal state specific heat data by fitting to $c_N(T) = \gamma_{exp}T + \beta T^3 + \delta T^5$ in which γ_{exp} is the Sommerfeld electronic specific heat coefficient and $\beta T^3 + \delta T^5$ are the first terms of the harmonic lattice approximation.
3) The electron-phonon coupling is calculated according to $\gamma_{exp} = (1+\lambda) \times \gamma_{comp}$
4) The predicted value in the weak coupling BCS limit is 1.426
5) The upper critical fields $\mu_0 H_{c2}$ for $T = 0$ are estimated from the midpoint values of T_c of the specific heat anomalies in zero and low magnetic fields by the Werthamer-Helfand-Hohenberg (WHH) extrapolation according to $\mu_0 H_{c2}(0) = -0.693\ T_c\ \mathrm{d}\mu_0 H_{c2}/\mathrm{d}T|_{T=Tc}$.
6) Superconducting volume fractions are not corrected for demagnetization effects.
7) The significantly smaller Meißner effects in the field-cooled samples are attributed to prominent flux-line pinning